Fitoterapia 179 (2024) 106217

Contents lists available at ScienceDirect

Fitoterapia

journal homepage: www.elsevier.com/locate/fitote

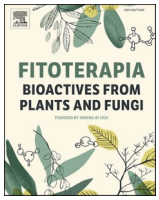

Bioactive abietenolide diterpenes from *Suregada procera*

Jackson Obegi Matundura [a,b], Jackson T. Mollel [c,d], Masum Miah [d], Joanna Said [d], Leonidah K. Omosa [a], Thobias M. Kalenga [e], Yannik T. Woordes [b], Vaderament-Alexe Nchiozem-Ngnitedem [a], Andreas Orthaber [f], Jacob O. Midiwo [a], Wouter Herrebout [g], Edward Trybala [d], Tomas Bergström [d], Luis Apaza Ticona [h], Mate Erdelyi [b,*], Abiy Yenesew [a,*]

[a] Department of Chemistry, University of Nairobi, P. O. Box 30197-00100 Nairobi, Kenya
[b] Department of Chemistry - BMC, Uppsala University, SE-751 23 Uppsala, Sweden
[c] Institute of Traditional Medicine, Muhimbili University of Health and Allied Sciences, P.O. Box 65001, Dar es Salaam, Tanzania
[d] Department of Infectious Diseases/Virology, Institute of Biomedicine, Sahlgrenska Academy, University of Gothenburg, S-413 46 Gothenburg, Sweden
[e] Department of Chemistry, College of Education, Mwalimu Julius K. Nyerere University of Agriculture and Technology, P.O. Box 976, Butiama, Tanzania
[f] Department of Chemistry - Ångström, Uppsala University, SE-751 20 Uppsala, Sweden
[g] Department of Chemistry, University of Antwerp, 2020 Antwerp, Belgium
[h] Department of Chemistry in Pharmaceutical Sciences, University Complutense of Madrid, Madrid, Spain

ARTICLE INFO

Keywords:
Suregada procera
Euphorbiaceae
Abietanolide
Antibacterial
Anti-inflammatory
Antitumoral

ABSTRACT

The phytochemical investigation of the leaves and the roots of *Suregada procera* afforded the new *ent*-abietane diterpenoid sureproceriolide A (**1**) along with the known secondary metabolites 8,14β:11,12α-diepoxy-13(15)-abietane-16,12-olid (**2**), jolkinolide A (**3**), jolkinolide E (**4**), *ent*-pimara-8(14),15-dien-19-oic acid (**5**), sitosterol (**6**), oleana-9(11):12-dien-3β-ol (**7**), and oleic acid (**8**). Their structures were elucidated by NMR spectroscopic and mass spectrometric analyses, and the structure of jolkinolide A (**3**) was confirmed by single-crystal X-ray diffraction analysis. Sureproceriolide A (**1**) showed modest activity against the Gram-positive bacterium *Staphylococcus lugdunensis* (MIC = 31.44 μM), and sitosterol (**6**) against the Gram-negative bacterium *Porphyromonas gingivalis* (IC_{50} = 45.37 μM). Jolkinolide A (**3**) and E (**4**) as well as sitosterol (**6**) inhibited the release of NOS (IMR-90 cells), TNF-α (HaCaT cells) and NF-κB (HaCaT cells), with IC_{50} values of 0.43, 3.21, and 10.32 μM, respectively. Compound **6** showed antitumoral activity against SK-MEL-28 (IC_{50} = 20.66 μM) and CCD-13Lu (IC_{50} = 24.70 μM) cell lines, with no cytotoxic effect against the prostate cells PrEC (CC_{50} > 300 μM).

1. Introduction

The genus *Suregada* (synonym *Gelonium*) belongs to the family Euphorbiaceae, which consists of *ca.* 40 species distributed widely in the tropics and subtropics, including Southeast Asia, Australia and Africa [1]. *Suregada lithoxyla* (Pax and K. Hoffim) Croizat, *S. procera* (Prain) Croizat and *S. zanzibariensis* Baill are found in East Africa [2], out of which the latter two are common in Kenya. *S. procera* is scattered across the Eastern Democratic Republic of Congo, South Sudan, Ethiopia, Zimbabwe, Mozambique and South Africa. A number of *Suregada* species have been used in traditional medicine for the management of ancylostomiasis, chest pain, gonorrhea [2], snake bites, stomachache, hernia, pneumonia [3], skin infections, abdominal upsets, asthma [4], malaria [5], purgative and hepatic disorders [6]. In addition, *S. procera* is used in traditional medicine in the management of hemorrhoids and gonorrhea [7], and its extracts show antiplasmodial [8,9] and anti-leishmanial [9,10] activities. Previous phytochemical investigation on the genus *Suregada* revealed the presence of diterpenoids [11], triterpenoids [12], flavonoids [13] and alkaloids [14]. Some of these secondary metabolites exhibit anticancer [3], antimalarial [15,16], antileishmanial and α-glucosidase inhibitory activities [14,17]. Mangiolide, isolated from *S. zanzibariensis*, displays antiplasmodial and antimicrobial activities [18].

Motivated by the scarce phytochemical information available on *S. procera*, a sparingly branched and evergreen shrub or tree that has a heavy and spreading crown and that reaches up to 24 m and that thrives

* Corresponding authors.
E-mail addresses: mate.erdelyi@kemi.uu.se (M. Erdelyi), ayenesew@uonbi.ac.ke (A. Yenesew).

https://doi.org/10.1016/j.fitote.2024.106217
Received 7 June 2024; Received in revised form 18 August 2024; Accepted 14 September 2024
Available online 18 September 2024

well in mixed evergreen, riverine and swampy forest at an altitude range of 300–2150 m above sea level, we investigated the secondary metabolites of its leaves and roots, and evaluated their antibacterial, anti-inflammatory, antitumoral, and antiviral activities.

2. Results and discussion

The CH_2Cl_2:MeOH (1:1) extract of *S. procera* (Prain) Croizat, also known *Gelonium procerum* Prain [19], was subjected to repeated silica gel chromatography and yielded one new (**1**) and seven known (**2**–**8**) compounds.

Compound **1** (Fig. 1) was obtained as white and amorphous solid. Its HRESIMS (Fig. S9, Supporting Information) exhibited a protonated molecular ion $[M + H]^+$ at *m/z* 349.1992 (calcd 349.2015) consistent with the molecular formula $C_{20}H_{28}O_5$, indicating seven degrees of unsaturation. The IR spectrum suggested the presence of hydroxy (3472 cm^{-1}) and carbonyl (1705 cm^{-1}, and 1741 cm^{-1}) groups. Its ^{13}C NMR spectrum (Table 1, Figs. S1-S7, Supporting Information) suggested a lactone [carbonyl (δ_C 173.0), vinylic methyl (δ_H 2.00, δ_C 9.7), α-C (δ_C 132.5) and β-carbon (δ_C 153.3)] of an abietane lactone skeleton, which is a common feature of plants belonging to the family Euphorbiaceae [2,20,21]. In addition, the ^{13}C NMR data showed the presence of an additional carbonyl (δ_C 197.5), an oxygenated quaternary carbon atom (δ_C 76.6), and an oxymethine (δ_H 4.52, δ_C 66.1) functionality. The ^{13}C NMR chemical shift values of ring C carbon atoms are similar to those reported for 3,4,18β-cyclopropa-8β-hydroxy-14-oxo-*ent*-abiet-13,15-en-16,12-olide [23], suggesting that one of the two hydroxy groups of compound **1** is placed at C-8 (δ_C 76.6), while the carbonyl (δ_C 197.5) is located at C-14. The HMBC correlations (Table 1) of CH_2–7 (δ_H 2.79 and 1.67) to C-9 (δ_C 57.0), and one of the C-11 protons (δ_H 2.12) to C-8 (δ_C 76.6) supported the placement of a hydroxy group at C-8 (δ_C 76.6). The placement of the C-14 carbonyl group at δ_C 197.5 was supported by the HMBCs of CH_2–7 (δ_H 2.79 and 1.67), to C-9 (δ_C 57.0) and C-14 (δ_C 197.5). The second hydroxy group was placed at C-6 (δ_C 66.1), based on the HMBCs of CH_2–7 (δ_H 2.79) and of H-5 (δ_H 1.01) to C-6 (δ_C 66.1). A comparison of its NMR data to those of known abietenolides in literature [20,21] suggested **1** to be a trioxygenated abietanolide, which possesses a carbonyl and two hydroxy functionalities in a 6/6/6/5 (rings A-D) *ent*-abietane diterpenoid architecture, similar to that of the mangiolide, which was reported from *S. zanzibariensis* [3,18]. The CSEACRH [22] predicted ^{13}C NMR chemical shifts (Table 1) for the proposed structure were in good agreement with most of the experimentally obtained values, confirming the above assignment. This data is consistent with 6,8-dihydroxy-14-keto-*ent*-abieta-13(15)-ene-16,12-olide.

The relative configuration of **1** was established based on NOESY correlations (Figs. 2 and S6, Supporting Information), vicinal coupling constants and biogenetic considerations. The fusion pattern of the A/B rings in *ent*-abietane diterpenoids is usually *trans* [6], with H-5 being β-oriented and CH_3–20 being α-oriented [24]. The small coupling constant $^3J_{5,6} < 1$ Hz between H-5_{ax} (δ_H 1.01) and H-6 (δ_H 4.52) indicated that H-6 is not axially oriented, but it is rather equatorial (β-oriented), similar to H-6 of mangiolide [3]; accordingly, OH-6 is α-oriented. This proposal was supported by the strong NOE correlation of H-6 (δ_H 4.52) with H-5 (δ_H 1.01), H-7β (δ_H 1.67) and CH_3–18 (δ_H 1.01, β-oriented) suggesting that these groups are all on the same face, and hence β-oriented. The unusual axial orientation of OH-6 is likely due to stabilization provided by an intermolecular hydrogen bond to the C-14 carbonyl oxygen (Fig. 2). The small $^3J_{5,6} < 1$ Hz coupling constant between H-5ax and H-6 eq may be attributed to the antiperiplanar arrangement of H-5ax and the axially oriented OH-6 depleting the electron density [25]. Similarly, NOE between CH_3–20 (δ_H 1.17) and H-12 (δ_H 5.47) showed that these protons are α-oriented and on the same face of the molecule. The strong NOE between H-5ax (δ_H 1.01) and H-9 (δ_H 1.98) indicated that H-9 is also axial. This reveals the B/C ring to be *cis*-fused, with OH-8 being β-oriented, similar to that of 3,4,18β-cyclopropa-8β-hydroxy-14-oxo-ent-abiet-13,15-en-16,12-olide [23] and related abietane lactone diterpenoids [3]. The ^{13}C NMR chemical shift values (Table 1) for the ring C carbon atoms are in close agreement with the chemical shifts of related abietane lactone diterpenoids with *cis*-fused B/C ring junction [23]. This new compound, sureproceriolide A (**1**), was therefore tentatively determined as 6α,8β-dihydroxy-14-keto-*ent*-abieta-13(15)-ene-16,12-olide.

The absolute configuration of **1** as shown in Fig. 1 was confirmed by DFT-based conformational analysis, and by comparing the predicted Boltzmann weighted ECD spectra with the experimental CD data (Fig. 3, and Figs. S13–14, Supporting Information).

The NMR data of compound **2** (Tables S1–2, Supporting Information)

Table 1
^{13}C (150 MHz) and ^1H (600 MHz) NMR data for Sureproceriolide A (**1**) in $CDCl_3$.

Position	**1**			
	$\delta_{C,\ type}$	$\delta_{C(calc)}$[a]	δ_H,*mult* (*J* in Hz)	HMBC, H → C
1a	43.3, CH_2	39.6	1.43 m	–
1b			1.17 m	–
2a	18.7, CH_2	18.6	1.66 m	–
2b			1.53 m	–
3a	43.7, CH_2	43.7	1.91 m	–
3b			1.08 m	–
4	33.1, C	33.6	–	–
5	56.6, CH	60.7	1.01 m	C-6, 10, 20
6	66.1, CH	67.2	4.52 s	–
7a	41.5, CH_2	44.0	2.78 d (14.1)	C-5, 6, 8, 9, 14
7b			1.67 d (14.1)	C-6, 8, 14
8	76.6, C	74.2	–	–
9	57.0, CH	50.3	1.98 m	C-1, 8, 10, 12, 14, 20
10	38.6[b], C	38.3	–	–
11a	26.8, CH_2	27.4	2.67 dd (13.8, 7.2)	C-8, 9, 12, 13
11b			2.12 m	C-9, 10, 12
12	80.1, CH	77.4	5.47 t (9.5, 9.5)	–
13	153.3[b], C	150.2	–	–
14	197.5[b], C	198.2	–	–
15	132.5[b], C	131.1	–	–
16	173.0[b], C	172.8	–	–
17	9.7, CH_3	9.4	2.00 s	C-13, 15, 16
18	34.3, CH_3	28.7	1.01 s	C-3, 5, 19
19	23.8, CH_3	28.7	1.20 s	C-3, 5, 18
20	22.2, CH_3	17.2	1.18 s	C-1, 5, 9, 10

[a] Calculated using CSEARCH [22].
[b] Signals observed in the HMBC spectrum.

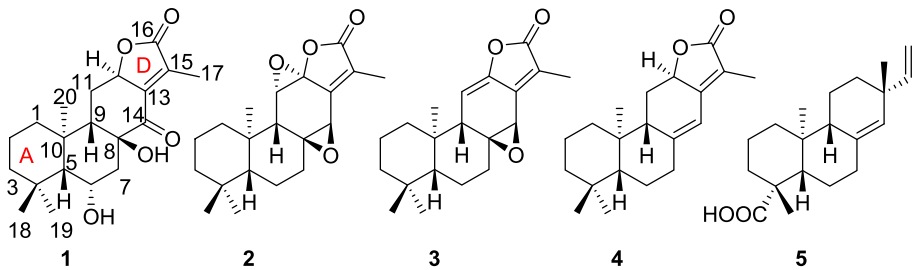

Fig. 1. The diterpenes isolated from the leaves and roots of *Suregada procera*.

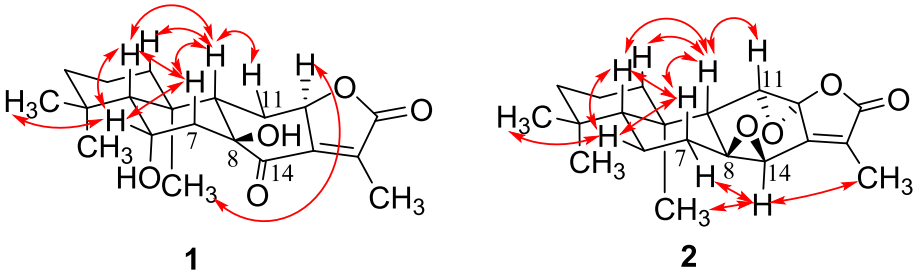

Fig. 2. Key NOESY correlations observed for compounds **1** and **2.**

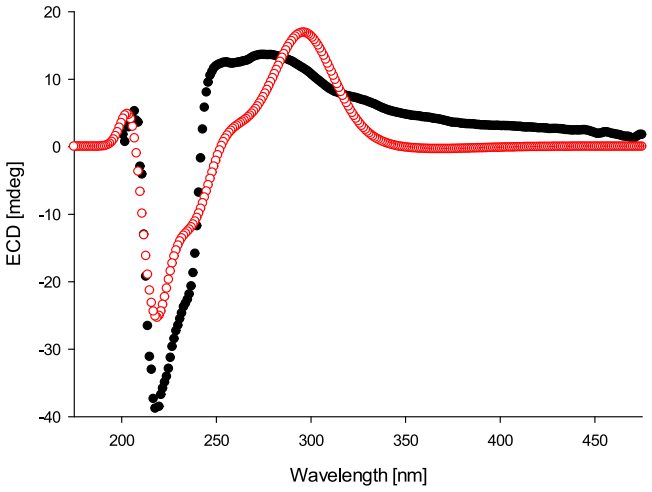

Fig. 3. The experimental ECD spectrum (methanol) of compound **1** (black) superimposed with that predicted (red). The similarity index describing the agreement between calculated and experimental data obtained using SpecDis [26,27] is 0.8779. (For interpretation of the references to colour in this figure legend, the reader is referred to the web version of this article.)

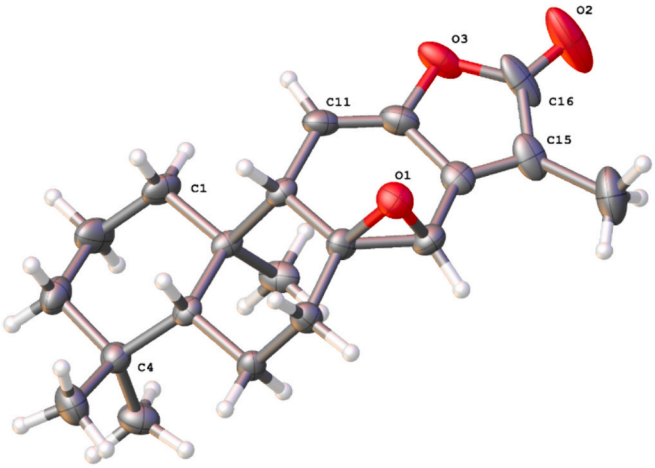

Fig. 4. Solid-state structure of jolkinolide A (**3**, CCDC 2361054). ORTEP-like plot with thermal ellipsoids shown at 50 % probability level.

is similar to those reported and computationally predicted for the diastereomeric 8,14β:11,12α-diepoxy-13(15)-abietane-16,12-olide (**2**) [18,28] and 8,14β:11,12β-diepoxy-13(15)-abietane-16,12-olide [3,29,30]. The NOE (Fig. 2) correlation of H-14 (δ_H 3.68) with the α-oriented Me-20 (δ_H 0.82) revealed that H-14 is α-oriented, which indicates that the epoxide at C-8/C-14 is β-oriented. The NOE between H-11 (δ_H 4.04) and H-9 (δ_H 2.29, which is β-oriented) revealed that H-11 is also β-oriented, and the epoxide at C-11/C-12 is hence α-oriented. This confirms relative configuration of **2** to be 8,14β:11,12α-diepoxy-13(15)-abietane-16,12-olide (Figs. 1–2). The diastereomer of this compound, 8,14β:11,12β-diepoxy-13(15)-abietane-16,12-olide, has been reported as jolkinolide B by Mangisa et al. from *Suregada zanzibariensis* [3,18].

Compound **3** was identified as jolkinolide A [31–33], based on NMR and MS analyses and by comparison of its spectroscopic data to those reported. Single-crystal X-ray diffraction analysis at 180 K using Mo Kα radiation (Fig. 4) established its structure unambiguously, confirming the relative configuration (5*R*,8*S*,9*S*,10*R*,14*R*)-8,14-epoxy-4,4,10,15-tetramethyl-1,2,3,5,6,7,9,11,14-decahydrophenanthro-[3,2-*b*]furan-16-one with final R^1 and wR^2 values of 5.73 % and 12.78 %, respectively. This solid state-structure of *ent*-abietane **3** is similar to that previously reported from room temperature data [34]. The configuration shown in Fig. 4 is as the other abietanolides of this plant, including the new compound **1**, being *ent*-abietanolides with trans-A/B and cis-B/C ring junctions. The additional isolated known compounds were identified as jolkinolide E (**4**) [33,35], *ent*-pimara-8(14),15-dien-19-oic acid (**5**) [36], sitosterol (**6**) [37], oleana-9(11):12-dien-3β-ol (**7**) [38], and oleic acid (**8**) [39] (Fig. 1, Tables S2-S8, Supporting Information).

The biological activities of compounds **2** [18] and **2a** (Section S2, Supporting Information) [40–42] have been previously documented. For instance, compound **2** has significant antimalarial (IC_{50} = 1.24 μg/mL), anticancer (IC_{50} = 3–14 μg/mL) and feeding deterrent activities against *T. castaneum* [3,18,30,43].

Compounds **1**, and **3**–**6** did not show cytotoxicity (CC_{50}) when evaluated against the HEKa, IMR-90, and HPrEC cell lines using Actinomycin D (ACTD, CC_{50} = 0.01 ± 0.001 μM) as positive standard [44] (Table 2). The cell viability for compounds **3**, **4**, **5**, and **6** have previously been investigated. Compound **3** preserves 100 % cell viability in the RAW264 cell line (mouse macrophages) at a concentration of 10 μM [45], **4** does not affect the viability of RAW264.7 cells up to a concentration of 50 μM [46], **5** shows a viability level of 60 % in the T1074 cell line (human ovarian epithelial cells) at 10 μM [47] and **6** a viability of 67.05 % in the NIH/3 T3 cell line (mouse embryonic fibroblasts) at a concentration of 2411 μM [48].

Comparing our results with previous data, we observed that abietanolides **1**, **3**, **4** and *ent*-pimara-8(14),15-dien-19-oic acid (**5**) have lower cytotoxicity as compared to the standard ACTD. This may indicate a potential specificity towards certain cell types, such as macrophages and ovarian cells. The significantly lower CC_{50} values observed on skin cells in this study, as compared to a previous study [48], may possibly be attributed to differences in experimental conditions or the characteristics of the cell lines used.

We explored the anti-inflammatory properties of the isolated compounds, focusing on their ability to modulate the production of proinflammatory cytokines [49]. The inhibition of TNF-α, NF-κB, and NO production were used as evaluation parameters, and compared to the positive controls C87 (IC_{50} = 0.06 ± 0.01 μM for TNF-α), Celastrol (IC_{50} = 7.76 ± 0.06 μM for NF-κB), and LNMMA (IC_{50} = 6.75 ± 0.28 μM for NO). All studied compounds showed inhibitory activity on TNF-α, NF-κB, and NO production, suggesting anti-inflammatory potential. The compounds tested here had a stronger effect on NO production than the

Table 2
Cytotoxicity and anti-inflammatory (TNF-α, NF-κB, and NO) activity at 72 h of the compounds isolated from *Suregada procera*.

Samples	HEKa				IMR-90				HPrEC			
	CC_{50} (μM)	TNF-α IC_{50} (μM)	NF-κB IC_{50} (μM)	NO IC_{50} (μM)	CC_{50} (μM)	TNF-α IC_{50} (μM)	NF-κB IC_{50} (μM)	NO IC_{50} (μM)	CC_{50} (μM)	TNF-α IC_{50} (μM)	NF-κB IC_{50} (μM)	NO IC_{50} (μM)
1	81.10	3.31	13.68	NA	81.40	4.97	17.34	NA	100.00	5.16	22.80	NA
3	77.20	3.55	13.58	0.46	80.20	5.15	17.56	0.43	81.70	6.74	22.68	0.54
4	76.80	3.21	13.14	2.72	79.80	4.29	17.84	2.98	82.90	6.21	22.80	3.50
5	82.90	4.36	10.58	2.19	83.20	5.34	14.93	2.95	83.90	6.83	18.00	3.62
6	80.50	11.33	10.32	NA	86.20	15.13	13.82	NA	>300	19.44	17.40	NA

HEKa: skin cells; IMR-90: lung cells; HPrEC: prostate cells; NA: The compounds were not active on the pharmacological targets. The experiments were performed in triplicate.

positive control LNMMA. Abietanolides **1**, **3**, and **4** exhibited similar inhibition of TNF-α and LPS-induced NF-κB in all evaluated cells. These compounds reduced TNF-α production (with IC_{50} 3.21–6.74 μM) more efficiently as compared to NF-κB (IC_{50} 13.14–22.80 μM) (Table 2). In contrast, **5** and **6** showed a higher capacity for NF-κB inhibition compared to the other studied compounds, with IC_{50} 10.58–18.00 μM and 11.33–19.44 μM, respectively. Compound **3** was the most active in NO inhibition (IC_{50} 0.43–0.54 μM), possibly due to its C8-C14 epoxide group [45]. In contrast, compounds **1** and **6** showed no activity on NO under our experimental conditions.

Our findings diverge from a previous study [45] reporting no anti-inflammatory activity (TNF-α and NO) for **3** in the RAW264 cells at 10 μM concentration, and from another [46] reporting anti-inflammatory activity (NO inhibition) for **4** in RAW264 cells at 20 μM concentration. Moreover, Suh et al. [50] reported **5** to negatively regulate the transcription or translation of MMP-9 by decreasing TNF-α stimulation in human aortic smooth muscle cells at 20 μM concentration, Sun et al. [51] reported **6** to have anti-inflammatory activity (TNF-α and NO inhibition) at 16 μM concentration in BV2 microglial cells that were derived from C57/BL6 mice. In our hands, we had no effect on NO was observed despite similar TNF-α inhibition values. These discrepancies may be due to variations in experimental conditions and the cell lines used. Nevertheless, further studies are needed to understand the mechanisms of action and the efficacy in preclinical and clinical models for these promising compounds.

To determine the *in vitro* antitumor activity, we conducted a double staining technique employing rhodamine 123 to detect changes in the mitochondrial membrane, and propidium iodide to identify necrotic cells using the positive control dimethylnastrone (IC_{50} = 0.21 ± 0.06 μM). The compounds exhibited *in vitro* antitumor activity, but none surpassed that of the positive control.

Compounds **1** and **3**–**6** had significant activity against SK-MEL-28 skin and CCD-13Lu lung cancer cells (Table 3), with IC_{50} 20.66–33.30 μM and 24.70–36.90 μM, respectively. Only compound **1** (IC_{50} = 35.14 μM) showed activity on VCaP prostate cancer cells similar to the positive control.

Previous studies indicated that compound **3** had antitumor activity on A549 human lung cancer cells at 63.66 μM concentration [52]. In our hands, **3** exhibited antitumor activity against the lung tumour cell line at half the reported concentration (33.70 μM). Compound **4** was reported to show cytotoxicity on A549 human lung cancer, MCF-7 human breast cancer, Mewo human melanoma, SH-SY5Y human neuroblastoma, Lovo human colon adenocarcinoma, and HepG2 human liver cancer) cell lines at concentrations >100 μM [53]. In our hands, **4** showed cytotoxic at 34.98 μM on lung tumour cells. Compound **5** was reported to be cytotoxic on PA-1 human ovarian cells at 20 μM concentration [47], and **6** to be cytotoxic on human hepatic cell lines Huh7 and HepG2 at 11.20 μM [54,55], comparable to the cytotoxicity observed by us on other cell lines (Table 3). The disparity in the IC_{50} values may be due to different exposure times, and to the nature of the assay, namely we performed assayed apoptotic capacity specifically, while previously viability assays (MTT, CC_{50}) were reported.

We evaluated the antibacterial potential of **1**, **3**–**6** against nine Gram-positive and three Gram-negative bacteria (Table 4), comparing the results to the positive control ofloxacin (MIC = 27.71 ± 2.05 μM). All studied compounds exhibited activity against the Gram-positive bacteria *K. rhizophila*, *S. lugdunensis*, and *S. mutans*, with MIC values 31.44–71.16 μM. Compound **1** had the highest activity (MIC = 31.44 μM) against the *S. lugdunensis* strain. All compounds exhibited activity against the Gram-negative *P. gingivalis* and *P. intermedia*, with **6** (MIC = 45.37 μM) showing the strongest activity against *P. gingivalis*.

Our results differ from previous reports in some aspects. For example, **3** was reported to be inactive against the Gram negative *Moraxella catarrhalis* > 300 μM [56], whereas in our hands the MIC values for Gram-negative bacteria ranged 66.76–72.40 μM, except the *N. gonorrhoeae* bacterial strain (Table 4), Compound **5** was reported to have antibacterial activity against the Gram-positive *Loque americana* (MIC 20.68 μM) [57], whereas we obtained MIC values >100 μM in some Gram-positive bacteria. Finally, **6** was reported to exhibit antibacterial activity against the Gram-positive *S. aureus* > 300 μM [58], whereas in our studies it showed activity at 100 μM against some Gram-

Table 3
Antitumor activity of the compounds isolated from *Suregada procera*.

Samples	IC_{50} (μM)		
	SK-MEL-28	CCD-13Lu	VCaP
1	23.50	27.90	35.14
3	26.30	33.70	>150
4	33.30	34.98	>200
5	28.37	36.90	>100
6	20.66	24.70	100.00

SK-MEL-28: skin tumour cells; CCD-13Lu: lung tumour cells; VCaP: prostate tumour cells. The experiments were performed in triplicate.

Table 4
Antibacterial (MIC, μM) activity of the compounds isolated from *Suregada procera*.

Bacterial strains	Samples (MIC in μM after 48 h)				
	1	**3**	**4**	**5**	**6**
Gram-positive bacteria					
A. viscosus ATCC 15987	>300	>250	>150	>100	100.00
B. subtilis ATCC 6051	>300	>250	>150	75.01	100.00
K. rhizophila ATCC 9341	43.09	42.37	42.83	49.68	53.45
L. monocytogenes ATCC 15313	>300	>250	>150	>100	100.00
M. sciuri ATCC 29062	64.61	>250	>150	>100	100.00
M. luteus ATCC 4698	59.03	>250	64.21	71.63	57.75
N. nova ATCC BAA-2227	>300	>250	>150	73.72	100.00
S. lugdunensis ATCC 43809	31.44	53.43	57.32	45.70	71.16
S. mutans ATCC 25175	69.34	62.66	67.67	61.37	57.01
Gram-negative bacteria					
N. gonorrhoeae ATCC 19424	77.17	>250	>150	>100	100.00
P. gingivalis ATCC 33277	66.92	66.76	70.06	58.98	45.37
P. intermedia ATCC 25611	70.66	72.40	77.10	58.58	60.98

The experiments were performed in triplicate.

positive bacteria. These differences are likely due to the different bacterial strains used in the studies.

Compounds **1** and **3**–**6** showed no anti-human rhinovirus type 2 (HRV-2) activity in the cytopathic effect reduction assay in HeLa cells (Supplementary Information, Table S12), no anti-respiratory syncytial virus (RSV) activity in the plaque reduction assay in HEp-2 cells (Supplementary Information, Table S13), and no anti-herpes simplex virus type 2 (HSV-2) activity in the plaque reduction assay in GMK AH1 cells (Supplementary Information, Table S14).

In conclusion, the phytochemical analysis of *S. procera* afforded the new *ent*-abietane diterpenoid sureproceriolide A (**1**) and seven known secondary metabolites (**2**–**8**). The isolated compounds showed weak antibacterial and antitumoral yet no antiviral activities, and some inhibited the production of NOS and the expression of TNF-α and NF-κB.

3. Materials and methods

3.1. General experimental procedures

Infrared (IR) measurements were recorded on a PerkinElmer spectrum FT-IR spectrometer using liquid samples. UV spectra were obtained using MeOH as the solvent on a Shimadzu UV-1650 PC UV/ vis spectrophotometer. Optical rotations were determined using a 341 LC OROT polarimeter at 589 nm and 24.0 °C, whereas ECD spectra were acquired on a JASCO *J*-810, Rev.1.00, spectropolarimeter. NMR spectra were acquired on an Agilent MR-400-DD2 400 MHz equipped with a 5 mm One NMR probe and on a Bruker Avance NEO 500 MHz equipped with TXO cryogenic probe or Bruker Avance 600 MHz equipped with TCI cryogenic probe spectrometers. The spectra were processed using Mestre Nova (v14.0.0) software referencing the carbon and proton chemical shifts to the residual deuterated solvent signals ($CDCl_3$: δ_H 7.26, δ_C 77.16; CD_3OD: δ_H 3.31, δ_C 49.00; CD_2Cl_2: δ_H 5.32, δ_C 53.84; DMSO-d_6: δ_H 2.50, δ_C 39.50) as internal standards. Assignments were based on 1D (^{1}H and ^{13}C) and 2D (HSQC, HMBC, COSY, NOESY and TOCSY) NMR spectra. The mass spectra were acquired on a waters micro-mass ZQ Multimode Ionization ESCI mode, connected to an Agilent 1100 series gradient pump system and a C18 Atlantis T3 column (3.0 × 50 mm, 5 μM), and using Milli-Q H_2O-MeOH (5:95 to 95:5, with 1 % HCO_2H and a flow rate of 0.75 mL/min over 7 min). HRESIMS spectra were obtained with a Q-TOF-LC/MS spectrometer using a 2.1 × 30 mm, 1.7 μM RPC_{18} and H_2O-CH_3CN gradient (5:95 to 95:5 in 0.2 % formic acid, *v*/v). Column chromatography was conducted on silica gel 60 (230–400 mesh) and on Sephadex LH-20 (GE Healthcare). Thin layer chromatography (TLC) analyses were performed on pre-coated silica gel 60 F_{254} aluminum plates (Merck, Darmstadt, Germany) using UV detection at 254 and 366 nm, followed by spraying with anisaldehyde reagent (prepared by mixing 3.5 mL of 4-anisaldehyde with 2.5 mL of concentrated sulfuric acid, 4 mL of glacial acetic acid, and 90 mL of methanol) and heated (80–100 °C). Preparative thin layer chromatography (PTLC) was conducted on squared glass plates of 20 × 20 cm, pre-coated with silica gel 60F_{254} having 0.25 to 1 mm thickness.

3.2. Plant material

The leaves and roots of *Suregada procera* were collected from the Ngong forest, Nairobi County, Kenya, in June 2019. The plant was authenticated by Mr. Patrick Charo Mutiso, a plant taxonomist of the Department of Biology, Faculty of Science and Technology, University of Nairobi, where a voucher specimen (JMOUON/2019/001) was deposited.

3.3. Extraction and isolation

The pulverized leaves (1.8 kg) of *Suregada procera* were extracted at room temperature with a 1:1 mixture of CH_2Cl_2/ MeOH (4 × 4 L, 24 h × 3), affording 210 g (12 %) of crude extract. A portion (80 g) of the extract was chromatographed over silica gel column (500 g) using pet. ether/EtOAc followed by EtOAc/MeOH mixtures, which yielded 8 sub-fractions (A-H). Sub-fraction A was separated by column chromatography over silica gel (30 g) and eluted with pet. ether/EtOAc (9.4:0.6, *v*/v) to yield **6** (7.0 mg) and **7** (3.0 mg). Following a previous procedure, sub-fraction B (pet. ether/EtOAc 9.2:0.8, v/v) afforded **5** (1.8 mg) and **3** (4.9 mg). Sub-fraction E (pet. ether/EtOAc 4:1, v/v) was purified on Sephadex LH-20 (CH_2Cl_2/MeOH 1:1) and further subjected to preparative TLC (*n*-hexane/EtOAc 6.5:3.5, v/v) yielding **1** (1.4 mg).

The dried and finely chopped roots (4.0 kg) were extracted as described above to afford 395 g (10 %) crude extract. Part of this extract (150 g) was subjected to gravity column chromatography over silica gel (1500 g) using *n*-hexane/CH_2Cl_2 gradient followed by CH_2Cl_2/MeOH to afford 10 sub-fractions (A-J). Sub-fraction H (*n*-hexane/CH_2Cl_2 1:4 v/v) was purified by column chromatography over Sephadex LH-20 (CH_2Cl_2/MeOH 1:1, v/v) and afforded **8** (6.2 mg). Sub-fraction I (*n*-hexane/CH_2Cl_2 1:9, v/v) yielded **2** (3.0 mg) and **4** (2.0 mg).

Sureproceriolide A (**1**). White amorphous solid, $[\alpha]^{24}{}_D + 42$ (c 3.3 × 10^{-4} $CHCl_3$), IR (neat, ν_{max}): 3472, 2929, 1741, 1705, 1468, 1062 cm^{-1}; ^{1}H and ^{13}C NMR data (Table1); HRESIMS *m/z* 349.1992 [M + H] $^+$ (Supporting information, Fig. S9) (calc. For $C_{20}H_{29}O_5$, 349.2015).

3.4. Biological assays

3.4.1. Cell culture reagents and drugs

HEKa (Human epidermal keratinocytes, PCS-200-011), SK-MEL-28 (Human melanocytes malignant melanoma, HTB-72), IMR-90 (Human lung fibroblast, CCL-186), CCD-13Lu (Human lung fibroblast carcinoma, CCL-200), HPrEC (Human prostate epithelial cell, PCS-440-010), and VCaP (Human prostate epithelial carcinoma, CRL-2876) were used in this study. All cell lines were obtained from the American Type Culture Collection (ATCC, USA).

The cells were cultivated in a Dulbecco's modified eagle medium (DMEM Sigma-Aldrich, CAS Number D5030) supplemented with 2 mM L-glutamine (≥ 99 % Sigma-Aldrich, CAS Number 56–85-9), 10 % fetal bovine serum (FBS Sigma-Aldrich, CAS Number TMS-016), 100 units/mL of penicillin and 100 μg/mL of streptomycin (Sigma-Aldrich, CAS Number P4333) in culture flasks. They were maintained in an incubator under normoxic conditions (20–21 % O_2) with humidified atmosphere (5 % CO_2, at 37 °C). In the case of tumour cells, hypoxic conditions (1 % O_2), were employed to mimic the *in vivo* tumour microenvironment.

The samples dilutions (100, 50, 25, 12.5, 6.25, 3.13, 1.56, 0.78, 0.39, and 0.20 μM) were prepared in a culture medium with 0.5 % dimethyl sulfoxide (DMSO ≥99.9 % Sigma-Aldrich, CAS Number 67–68-5) from stock solutions at a concentration of 1 mM by dissolving them in DMSO. To determine the cytotoxicity of the vehicle (DMSO-negative control), culture medium with 0.5 % DMSO was added to the cells at the corresponding proportions of the sample solutions.

3.4.2. Cytotoxicity assay

Cell viability was measured using a colorimetric assay in 96-well plates with 2-(4-iodophenyl)-3-(4-nitrophenyl)-5-(2,4 disulfophenyl)-2*H*-tetrazolium monosodium salt (WST-1 Sigma-Aldrich, CAS Number 5015944001) reagent [59]. Each plate included blanks (untreated cells), the Actinomycin D positive control (ACTD ≥95 % Sigma-Aldrich, CAS Number 50–76-0), and sample dilutions at different concentrations with three replicates each.

For the HEKa, IMR-90 and HPrEC cells, dilution series of the tested samples in medium were prepared in 96-well plates. Cells (3×10^3 cells/mL in DMEM with 8 % FSB) were added to the plates and incubated for 72 h. After 72 h, 10 μL of WST-1 (diluted 1:4 with phosphate buffer) was added, and cells were further incubated for another 4 h. Cell viability was measured at 450 nm in a spectrophotometric enzyme-linked immunosorbent assay (ELISA) microplate reader (Anthos 2020, Version 2.0.5, Biochrom Ltd., UK).

3.4.3. Anti-inflammatory assay

3.4.3.1. TNF-α inhibition assay. The cells (5×10^4 cells/well) were seeded on a 96-well culture plate and incubated for 12 h. Subsequently, the cells were pre-treated with various concentrations of the samples for 2 h before stimulation with 0.1 μg/mL of lipopolysaccharide (LPS Sigma-Aldrich, CAS Number L8274) with or without samples for 72 h. Supernatants were collected, and the protein expression levels of TNF-α were measured using an ELISA kit, following the manufacturer's instructions (Diaclone Company, Besancon, France) [60]. Absorbance was read at 450 nm on a spectrophotometric ELISA plate reader (Anthos 2020, Version 2.0.5, Biochrom Ltd., UK). The percentage of TNF-α inhibition was calculated from the ratio between the observed TNF-α amount secreted by treated cells (μM) and the baseline secretion of TNF-α (pg/mL). C87 (Sigma-Aldrich, CAS Number 332420–90-3) was used as positive control.

3.4.3.2. NF-κB inhibition assay. All cells were stably transfected with the KBF-Luc plasmid, which contains three copies of the NF-κB binding site (from the major histocompatibility complex promoter) fused to a minimal simian virus 40 promoter driving the luciferase gene. Cells (3×10^3 for cells/well) were seeded the day before the assay in a 96-well plate. Subsequently, the cells were treated with samples at the same concentrations used in the viability assays for 15 min, followed by stimulation with 0.1 μg/mL of lipopolysaccharide (LPS Sigma-Aldrich, CAS Number L8274) [59]. Celastrol (≥ 98 % Sigma-Aldrich, CAS Number 34157–83-0) was used as a positive control. After 72 h, the cells were washed twice with PBS and lysed in 50 μL lysis buffer containing 25 mM Tris-phosphate (pH 7.8), 8 mM $MgCl_2$, 1 mM DL-dithiothreitol (DTT Sigma-Aldrich, CAS Number 3483–12-3), 1 % Triton ™ X-100 (Sigma-Aldrich, CAS Number 9036–19-5), and 7 % glycerol (≥ 99.5 % Sigma-Aldrich, CAS Number 56–81-5) for 15 min at room temperature (25 °C) on a horizontal shaker. Luciferase activity was measured using a microplate reader (Anthos 2020, Version 2.0.5, Biochrom Ltd., UK) following the instructions of the luciferase assay kit (Promega, Madison, WI, USA). The relative luminescence units (RLU) were calculated, and the results were expressed as the percentage of inhibition of NF-κB activity induced by TNF-α (100 % activation). The experiments for each concentration of the test elements were performed in triplicate wells.

3.4.3.3. NO inhibition assay. The cells (200 μL, 3×10^3 cells/well) were incubated with different concentrations (for details, please see the viability assay) of the samples for 2 h and then stimulated with 100 μg/mL LPS for 72 h to assess nitric oxide (NO) production. Griess reagent (Nitrite assay kit, Sigma-Aldrich, CAS Number G4410) was added to 50 μL of cultured supernatant and mixed for 10 min at room temperature (25 °C). Absorbance was measured at 540 nm. A sodium nitrite standard (≥ 97.0 % Sigma-Aldrich, CAS Number 7632-00-0) curve was used to calculate nitrite concentration. N^G-Methyl-L-arginine acetate salt (LNMMA ≥98 % Sigma-Aldrich, CAS Number 53308–83-1) was used as a positive control.

3.4.4. Antitumor assay

Apoptosis was determined using the rhodamine method with double staining (rhodamine 123 to detect changes in the mitochondrial membrane and propidium iodide to detect necrotic cells). Cells (20×10^4) were seeded in 55 mm plates with 2 mL of complete DMEM and treated with the samples at a concentration obtained by the viability assay WST-1 (CC_{50}). After 72 h of treatment, cells were incubated with 5 μL of rhodamine 123 (Rh123 Sigma-Aldrich, CAS Number 62669–70-9) (1 μg/μL) for 30 min. All cells in each well were harvested and centrifuged at 500 *g* for 10 min. The cell pellet was washed three times with 1 mL of PBS 1× + 1 % bovine serum albumin (BSA Sigma-Aldrich, CAS Number 9048-46-8) solution and resuspended in 500 μL of PBS 1× + 1 % BSA solution containing 0.5 μL of propidium iodide (PI Sigma-Aldrich, CAS Number 25535–16-4) (5 μg/μL). The entire procedure was performed at 4 °C [61]. The samples were analyzed by flow cytometry using the BD-FACSCalibur™ cytometer (Becton Dickinson BioScience, San Jose, CA, USA). The Expo32 software was used to analyse the data. The percentage of Rh123-negative and PI-negative cells corresponded to the apoptotic population. Dimethylenastron ($C_{16}H_{18}N_2O_2S$ Sigma-Aldrich, CAS Number 863774–58-7) was used as a positive control.

3.4.5. Antibacterial assay

3.4.5.1. Bacteria. The bacterial strains used include Gram-positive bacteria: *Actinomyces viscosus* (*A. viscosus,* ATCC 15987), *Bacillus subtilis* (*B. subtilis,* ATCC 6051), *Kocuria rhizophila* (*K. rhizophila,* ATCC 9341), *Listeria monocytogenes* (*L. monocytogenes,* ATCC 15313), *Mammaliicoccus sciuri* (*M. sciuri,* ATCC 29062), *Micrococcus luteus* (*M. luteus,* ATCC 4698), *Nocardia nova* (*N. nova,* ATCC BAA-2227), *Staphylococcus lugdunensis* (*S. lugdunensis,* ATCC 43809), and *Streptococcus mutans* (*S. mutans,* ATCC 25175); and Gram-negative bacteria: *Neisseria gonorrhoeae* (*N. gonorrhoeae,* ATCC 19424), *Porphyromonas gingivalis* (*P. gingivalis,* ATCC 33277), and *Prevotella intermedia* (*P. intermedia,* ATCC 25611).

3.4.5.2. Broth microdilution method. The minimum inhibitory concentration (MIC) of the samples against the bacteria was determined using the microdilution method in 96-well plates (Cellstar®, Greinerbio-one, Germany). Mueller-Hinton broth (MHB Sigma-Aldrich, CAS Number 90922) medium (180 μL) of the bacterial culture was used to fill the first experimental well. The remaining wells were filled with 100 μL of medium each. Subsequently, 20 μL of samples dilutions at different concentrations were added to the first well. A double-fold serial dilution was then carried out across the plate. An overnight batch culture of the bacteria (10 μL) was used to inoculate each well to achieve an inoculum size of *ca.* 1×10^6 colony-forming unit (CFU)/mL. The plates were incubated for 72 h at 37 °C [62]. DMSO was used as a negative control at the same concentration as the samples, while ofloxacin (≥ 99.9 % Sigma-Aldrich, CAS Number 82419–36-1) was used as positive control to assess the accuracy of the MIC method. Each MIC determination was carried out in triplicate.

3.4.6. Antiviral assay

The antiviral activity of the samples was evaluated against respiratory syncytial virus (RSV) in HEp-2 cells and against herpes simplex virus type 2 (HSV-2) in GMK AH1 cells by the viral plaque number reduction assay. The assay was conducted as described previously for RSV [52,63] and HSV-2 [53,64]. Briefly, a day prior to the experiments, the cells were seeded in a 24 well cluster plates to attain ~70–90 % confluence. Then the cells were rinsed with 300 μL of maintenance medium followed by addition of 400 μL of fresh medium and 50 μL of 5-fold serial dilutions of the test compounds in the medium. Following incubation for 15 min at 37 °C in a humidified atmosphere of 5 % CO_2 (CO_2 incubator) 50 μL of medium comprising 100 plaque forming units (PFU) of the virus was added and incubated for 1.5 h (HSV-2) or 2.5 h (RSV) in the CO_2 incubator. The virus-test sample mixture was aspirated and 750 μL of 0.75 % methylcellulose solution comprising the same concentration of the test compound was added and incubated for three days in the CO_2 incubator. The cells were then stained with 1 % solution of crystal violet to visualize the viral plaques. Anti-human rhinovirus type 2 (HRV-2) activity of test compounds was performed by the virus cytopathic effect reduction assay as described previously [65].

3.4.7. Statistical analysis

Data were analyzed using Prism v9.0.0 (Software LLC from 1994 to 2020). The data were normalised and plotted, computing the % activity *versus* the log of the compound concentration. The values of 50 % cytotoxic concentration (CC_{50}) and 50 % inhibitory concentration (IC_{50})

were calculated using the sigmoidal dose-response function. Additionally, a one-way ANOVA statistical analysis was performed to determine if the differences between the obtained values were statistically significant ($p < 0.05$; $p < 0.001$, Tukey's multiple comparisons test).

3.5. Optical spectroscopy

3.5.1. Optical spectroscopy

UV absorbance and ECD spectra were collected simultaneously on a 0.02 mg/mL sample in MeOH using a path length of 10 mm on a JASCO J-810 spectrophotometer. The solvent spectra were recorded under identical conditions to remove solvent bands in the UV spectra, and to baseline correct the ECD spectra.

3.5.2. Calculations

A low energy conformation library of postulated compound **1** was created using PC Model with the incorporated MMFF94 force field. All conformers within a cut-off of 5 kcal/mol from the lowest energy conformer were retained and subjected to DFT optimization and spectral calculations at the B3LYP/6–31++G(d,p) level of theory. Subsequently, for all conformations exhibiting an enthalpy-based Boltzmann weight higher than 0.1 %, UV and ECD spectra were obtained at the cam-B3LYP/6–311++G(d,p) level. The UV–vis and ECD spectra for the individual conformations were created by applying a Lorentzian broadening with full half width at half maximum of 10 cm^{-1}.

All DFT level calculations were performed using the Gaussian 16 software package with tight convergence criteria and ultrafine integration grids. For all calculations, solvent effects were implicitly taken into account using the IEFPCM model as implemented in the Gaussian suite.

3.6. X-ray diffraction analysis

Single crystals were obtained by slow solvent evaporation and were mounted on a fiber loop and fixated using Fomblin oil. SC-XRD measurements were performed using graphite-monochromatized Mo Kα radiation using a Bruker D8 APEX-II equipped with a CCD camera. Data reduction was performed with SAINT. Absorption corrections for the area detector were performed using SADABS. The structure was solved by direct methods and refined by full-matrix least-squares techniques against F2 using all data (SHELXT, SHELXS). All non-hydrogen atoms were refined with anisotropic displacement parameters if not stated otherwise. Hydrogen atoms constrained in geometric positions to their parent atoms using OLEX2. The structure of compound **3** (CCDC 2361054) has been deposited with the Cambridge Crystallographic Data Centre. Further details of the X-ray data acquisition are given in the Supplementary Information.

Funding

This research was funded by the Swedish Research Council (2019–03715 and 2018–03918), Sweden.

CRediT authorship contribution statement

Jackson Obegi Matundura: Writing – original draft, Investigation, Formal analysis. **Jackson T. Mollel:** Formal analysis. **Masum Miah:** Investigation, Formal analysis. **Joanna Said:** Writing – review & editing, Supervision, Investigation, Formal analysis. **Leonidah K. Omosa:** Supervision, Resources. **Thobias M. Kalenga:** Formal analysis, Data curation. **Yannik T. Woordes:** Writing – review & editing, Formal analysis, Data curation. **Vaderament-Alexe Nchiozem-Ngnitedem:** Investigation, Formal analysis. **Andreas Orthaber:** Writing – review & editing, Visualization, Investigation, Formal analysis. **Jacob O. Midiwo:** Supervision. **Wouter Herrebout:** Writing – review & editing, Visualization, Methodology, Formal analysis. **Edward Trybala:** Writing – review & editing, Methodology, Investigation, Formal analysis. **Tomas Bergström:** Writing – review & editing, Supervision. **Luis Apaza Ticona:** Writing – review & editing, Methodology, Investigation, Formal analysis. **Mate Erdelyi:** Writing – review & editing, Supervision, Resources, Project administration, Funding acquisition, Conceptualization. **Abiy Yenesew:** Writing – review & editing, Supervision, Formal analysis, Conceptualization.

Declaration of competing interest

The authors declare no conflict of interest. The funders had no role in the design of the study; in the collection, analyses, or interpretation of data; in the writing of the manuscript, or in the decision to publish the results.

Acknowledgements

We are grateful to the Swedish Research Council (2019–03715) and to the International Science Program (ISP-Sweden) for financial support. This study made use of the NMR Uppsala infrastructure, which is funded by the Department of Chemistry-BMC and the Disciplinary Domain of Medicine and Pharmacy. Mr. Patrick Charo Mutiso of the Herbarium, Faculty of Science and Technology, University of Nairobi is appreciated for authentication and collection of the plant material.

Appendix A. Supplementary data

NMR, MS, UV–vis and CD data for the isolated compounds and details of the antibacterial, antiviral and cytotoxicity assays (PDF). The original FIDs for compounds **1**–**8** are freely available on Zenodo (DOI: https://doi.org/10.5281/zenodo.10902897).

References

[1] R.Y. Yan, Y.X. Tan, X.Q. Cui, R.Y. Chen, D.Q. Yu, Diterpenoids from the roots of *Suregada glomerulata*, J. Nat. Prod. 71 (2008) 195–198, https://doi.org/10.1021/np0705211.

[2] T.M. Kalenga, J.T. Mollel, J. Said, A. Orthaber, J.S. Ward, Y. Atilaw, D. Umereweneza, M.M. Ndoile, J.J.E. Munissi, K. Rissanen, E. Trybala, T. Bergström, S.S. Nyandoro, M. Erdelyi, Modified *ent*-Abietane diterpenoids from the leaves of *Suregada zanzibariensis*, J. Nat. Prod. 85 (2022) 2135–2141, https://doi.org/10.1021/acs.jnatprod.2c00147.

[3] M. Mangisa, V.J. Tembu, G. Fouche, R. Nthambeleni, X. Peter, M.K. Langat, *Ent*-abietane diterpenoids from *Suregada zanzibariensis* Baill. (Euphorbiaceae), their cytotoxic and anticancer properties, Nat. Prod. Res. 33 (2019) 3240–3247, https://doi.org/10.1080/14786419.2018.1470628.

[4] E. Innocent, C.C. Joseph, N.K. Gikonyo, M.H.H. Nkunya, A. Hassanali, Constituents of the essential oil of *Suregada zanzibariensis* leaves are repellent to the mosquito, *Anopheles gambiae* s.s, J. Insect Sci. 10 (2010) 1–8, https://doi.org/10.1673/031.010.5701.

[5] E. Omulokoli, B. Khan, S.C. Chhabra, Antiplasmodial activity of four Kenyan medicinal plants, J. Ethnopharmacol. 56 (1997) 133–137, https://doi.org/10.1016/S0378-8741(97)01521-3.

[6] I.A. Jahan, N. Nahar, M. Mosihuzzaman, F. Shaheen, M.I. Choudhary Atta-ur-Rahman, Six new diterpenoids from *Suregada multiflora*, J. Nat. Prod. 67 (2004) 1789–1795, https://doi.org/10.1021/np020435v.

[7] F. Amare, G. Getachew, An ethnobotanical study of medicinal plants in chiro district, west Hararghe, Ethiopia, African J. Plant Sci. 13 (2019) 309–323, https://doi.org/10.5897/ajps2019.1911.

[8] N.M. Aljamali, Z.H. Al-zubaidy, A.H. Enad, Bacterial infection and common bacterial diseases: a review, Pharm. Nanotechnol. 3 (2021) 13–23.

[9] E.V.M. Kigondua, G.M. Rukunga, J.M. Keriko, W.K. Tonui, J.W. Gathirwa, P. G. Kirira, B. Irungu, J.M. Ingonga, I.O. Ndiege, Anti-parasitic activity and cytotoxicity of selected medicinal plants from Kenya, J. Ethnopharmacol. 123 (2009) 504–50963, https://doi.org/10.1016/j.jep.2009.02.008.

[10] I. Muhammad, J. Midiwo, B.L. Tekwani, V. Samoylenko, R. Sahu, F. Machumi, A. A. Rahman, L.A. Walker, J.P. Hester, Antileishmanial Activity of Kenyan Medicinal Plants, University of Nairobi, Nairobi, Kenya, 2008, pp. 1–2, https://doi.org/10.1055/s-0031-1273576.

[11] R. Yan, R. Chen, D. Yu, Two new diterpenoids from *Suregada glomerulata* (Blume) Baill, Chin. Chem. Lett. 22 (2011) 580–582, https://doi.org/10.1016/j.cclet.2010.12.015.

[12] P. Sathish Kumar, M.B.G. Viswanathan, M. Venkatesan, K. Balakrishna, Bauerenol, a triterpenoid from Indian *Suregada angustifolia*: induces reactive oxygen species–mediated P38MAPK activation and apoptosis in human hepatocellular carcinoma (HepG2) cells, Tumour Biol. 39 (2017) 1–15, https://doi.org/10.1177/1010428317698387.

[13] N. Parveen, N.U. Khan, Luteolin 7,4′-dimethyl ether 3′-glucoside from *Gelonium multiflorum*, Phytochemistry 26 (1987) 2130–2131, https://doi.org/10.1016/S0031-9422(00)81781-1.

[14] R.Y. Yan, H.Q. Wang, C. Liu, R.Y. Chen, D.Q. Yu, Three new water-soluble alkaloids from the leaves of *Suregada glomerulata* (Blume) Baill, Fitoterapia 82 (2011) 247–250, https://doi.org/10.1016/j.fitote.2010.10.004.

[15] D.D. Soejarto, C. Gyllenhaal, M.R. Kadushin, B. Southavong, K. Sydara, S. Bouamanivong, M. Xaiveu, H.J. Zhang, S.G. Franzblau, G.T. Tan, J.M. Pezzuto, M.C. Riley, B.G. Elkington, D.P. Waller, An ethnobotanical survey of medicinal plants of Laos toward the discovery of bioactive compounds as potential candidates for pharmaceutical development, Pharm. Biol. 50 (2012) 42–60, https://doi.org/10.3109/13880209.2011.619700.

[16] M. Noronha, V. Pawar, A. Prajapati, R.B. Subramanian, A literature review on traditional herbal medicines for malaria, South Afr. J. Botany. 128 (2020) 292–303, https://doi.org/10.1016/j.sajb.2019.11.017.

[17] R.Y. Yan, H.Q. Wang, C. Liu, J. Kang, R.Y. Chen, α-Glucosidase-inhibitory iminosugars from the leaves of *Suregada glomerulata*, Bioorg. Med. Chem. 21 (2013) 6796–6803, https://doi.org/10.1016/j.bmc.2013.07.048.

[18] J.O. Matundura, J.O. Midiwo, A. Yenesew, L.K. Omosa, M. Kumarihamy, J. Zhao, M. Wang, S. Tripathi, S. Khan, V.M. Masila, V.-A. Nchiozem-Ngnitedem, I. Muhammad, Antiplasmodial and antimicrobial activities of *ent*-abietane diterpenoids from the roots of *Suregada zanzibariensis*, Nat. Prod. Res. (2022) 1–5, https://doi.org/10.1080/14786419.2022.2158463.

[19] POWO, Plants of the World Online, Facilitated by the Royal Botanic Gardens, Kew, 2024. Published on the Internet, https://powo.science.kew.org/. Retrieved 14 August 2024, https://doi.org/10.1016/j.jenvman.2024.122468.

[20] C. Liu, Z.X. Liao, S.J. Liu, Y.B. Qu, H.S. Wang, Two new diterpene derivatives from *Euphorbia lunulata* Bge and their anti-proliferative activities, Fitoterapia 96 (2014) 33–38, https://doi.org/10.1016/j.fitote.2014.03.016.

[21] Q.C. Wu, Y.P. Tang, A.W. Ding, F.Q. You, L. Zhang, J.A. Duan, ^{13}C-NMR data of three important diterpenes isolated from *Euphorbia* species, Molecules 14 (2009) 4454–4475, https://doi.org/10.3390/molecules14114454.

[22] N. Haider, W. Robien; http://nmrpredict.orc.univie.ac.at/c13robot/robot.php.

[23] H. Haba, C. Lavaud, A.A. Magid, M. Benkhaled, Diterpenoids and triterpenoids from *Euphorbia retusa*, J. Nat. Prod. 72 (2009) 1258–1264, https://doi.org/10.1021/np900127j.

[24] R.J. Peters, Two rings in them all: the labdane-related diterpenoids, Nat. Prod. Rep. 27 (2010) 1521–1530, https://doi.org/10.1039/c0np00019a.

[25] B. Coxon, Developments in the Karplus equation as they relate to the NMR coupling constants of carbohydrates, Adv. Carbohydr. Chem. Biochem. 62 (2009) 17–82, https://doi.org/10.1016/S0065-2318(09)00003-1.

[26] E. Debie, E. De Gussem, R.K. Dukor, W. Herrebout, L.A. Nafie, P. Bultinck, A confidence level algorithm for the determination of absolute configuration using vibrational circular dichroism or Raman optical activity, ChemPhysChem 1-25 (2011) 1542.

[27] T. Bruhn, A. Schaumlöffel, Y. Hemberger, G. Bringmann, SpecDis: quantifying the comparison of calculated and experimental electronic circular dichroism spectra, Chirality 25 (2013) 243–249, https://doi.org/10.1002/chir.22138.

[28] S.K. Talapatra, G. Das, B. Talapatra, Stereostructures and molecular conformations of six diterpene lactones from *Gelonium multiflorum*, Phytochemistry 28 (1989), 4, 1181-l 185. doi:https://doi.org/10.1016/0031-9422(89)80205-5.

[29] X.C. Liu, L. Zhou, Z.L. Liu, Evaluation of nematicidal activity of ethanol extracts of Euphorbiaceae plants and constituents from *Euphorbia fischeriana* to *Meloidogyne incognita* (Kofoid and White) Chitwood, J. Ent. Zool. Stud. 2 (4) (2014) 311–317.

[30] Z.F. Geng, Z.L. Liu, C.F. Wang, Q.Z. Liu, S.M. Shen, Z.M. Liu, S.S. Du, Z.W. Deng, Feeding deterrents against two grain storage insects from *Euphorbia fischeriana*, Molecules 16 (2011) 466–476, https://doi.org/10.3390/molecules16010466.

[31] H. Wang, Z. Xiao-Fenga, C. Xiang-Haib, M.A. Yun-Baob, L. Xiao-Dong, Three new diterpenoids from *Euphorbia wallichii*, Chin. J. Chem. 22 (2004) 199–202, https://doi.org/10.1002/cjoc.20040220219.

[32] D. Uemura, Y. Hirata, Two new diterpenoids, jolkinolides a and B, obtained from *Euphorbia jolkini* Boiss. (Euphorbiaceae), Tetrahedron Lett. 15 (1972), 1587–1390.

[33] A.R. Lal, R.C. Cambie, T.P.S. Rutledge, P.D. Woodgate, *ent*-pimarane and *ent*-abietane diterpenes from *Euphorbia fidjiana*, Phytocheraistry 29 (7) (1990) 2239–2246.

[34] P. Hoet, I. Landa, M. Rivera, M. van Meerssche, G. Germain, J.P. Declercq, Crystal structure of jolkinolide a from *Euphorbia huachangana* (Kl & Gke) Boiss, Bull. Soc. Chim. Belg. 89 (1980) 385–388, https://doi.org/10.1002/BSCB.19800890509.

[35] N. Crespi-Perellino, L. Garofano, E. Arlandini, V. Pinciroli, A. Minghetti, F. F. Vincieri, B. Danieli, Identification of new diterpenoids from *Euphorbia calyptrata* cell cultures, J. Nat. Prod. 59 (1996) 773–776, https://doi.org/10.1021/np960127v.

[36] O.H. Kang, H.S. Chae, J.G. Choi, Y.C. Oh, Y.S. Lee, J.H. Kim, M.J. Seung, H.J. Jang, K.H. Bae, J.H. Lee, D.W. Shin, D.Y. Kwon, *Ent*-pimara-8(14), 15-dien-19-oic acid isolated from the roots of *Aralia cordata* inhibits induction of inflammatory mediators by blocking NF-κB activation and mitogen-activated protein kinase pathways, Eur. J. Pharmacol. 601 (2008) 179–185, https://doi.org/10.1016/j.ejphar.2008.10.012.

[37] W.R.P. Erwin, R.D. Safitry, E. Marliana, I.W. Kusuma Usman, Isolation and characterization of stigmasterol and 3β-sitosterol from wood bark extract of *Baccaurea macrocarpa* miq, Mull. Arg. Rasayan J. Chem. 13 (2020) 2552–2558, https://doi.org/10.31788/RJC.2020.1345652.

[38] R. Tanaka, S. Matsunaga, Triterpene dienols and other constituents from the bark of *Phyllanthus flexuosus*, Phytochemistry 27 (1988) 2213–2217.

[39] D. Malarvizhi, P. Anusooriya, P. Meenakshi, S. Sundaram, E. Oirere, V. K. Gopalakrishnan, Isolation, structural characterization of oleic acid from *Zaleya decandra* root extract, Anal. Chem. Lett. 6 (2016) 669–677, https://doi.org/10.1080/22297928.2016.1238319.

[40] Y.Y. Zhang, Y. Yan, J. Zhang, C.Y. Xia, W.W. Lian, W.P. Wang, J. He, W.K. Zhang, J.K. Xu, Jolkinolide B: a comprehensive review of its physicochemical properties, analytical methods, synthesis and pharmacological activity, Phytochemistry 204 (2022) 113448, https://doi.org/10.1016/j.phytochem.2022.113448.

[41] J.H. Wang, Y.J. Zhou, X. Bai, P. He, Jolkinolide B from *Euphorbia fischeriana* Steud1 induces apoptosis in human leukemic U937 cells through PI3K/Akt and XIAP pathways, Mol. Cell 32 (2011) 451–457, https://doi.org/10.1007/S10059-011-0137-0.

[42] Y. Wang, D. Sun, Q. Jiang, L. Xiong, N. Zhang, Y. Pan, H. Li, L. Chen, Diterpenoids with anti-inflammatory activity from *Euphorbia wallichii*, Phytochemistry 205 (2023) 113486, https://doi.org/10.1016/j.phytochem.2022.113486.

[43] W.K. Liu, J.C.K. Ho, G.W. Qin, C.T. Che, Jolkinolide B induces neuroendocrine differentiation of human prostate LNCaP cancer cell line, Biochem. Pharmacol. 63 (2002) 951–957, https://doi.org/10.1016/S0006-2952(01)00938-8.

[44] L. Apaza Ticona, B. Souto Pérez, V. Martín Alejano, Anti-inflammatory and anti-arthritic activities of glycosylated flavonoids from *Syzygium jambos* in Edematogenic agent-induced paw edema in mice, Rev. Bras (2021) 1–13, https://doi.org/10.1007/s13187-021-02063-6.

[45] T. Uto, G.W. Qin, O. Morinaga, Y. Shoyama, 17-Hydroxy-jolkinolide B, a diterpenoid from *Euphorbia fischeriana*, inhibits inflammatory mediators but activates heme oxygenase-1 expression in lipopolysaccharide-stimulated murine macrophages, Int. Immunopharmacol. 12 (1) (2012) 101–109, https://doi.org/10.1016/j.intimp.2011.10.020.

[46] Y. Wang, D. Sun, Q. Jiang, L. Xiong, N. Zhang, Y. Pan, H. Li, L. Chen, Diterpenoids with anti-inflammatory activity from *Euphorbia wallichii*, Phytochemistry 205 (2023) 113486, https://doi.org/10.1016/j.phytochem.2022.113486.

[47] W. Li, G. Xuemei, Z. Yilin, W. Han, H. Yajun, H. Yi, Z. Zhongxiang, Anticancer effects of Pimaric acid is mediated via endoplasmic reticulum stress, caspase-dependent apoptosis, cell cycle arrest, and inhibition of cell migration in human ovarian cancer cells, Acta Biochim. Pol. 69 (1) (2022) 245–250, https://doi.org/10.18388/abp.2020_6011.

[48] M. Ayaz, A. Sadiq, A. Wadood, M. Junaid, F. Ullah, N. Zaman Khan, Cytotoxicity and molecular docking studies on phytosterols isolated from *Polygonum hydropiper* L, Steroids 141 (2019) 30–35, https://doi.org/10.1016/j.steroids.2018.11.005.

[49] V.-A. Nchiozem-Ngnitedem, L.K. Omosa, K.G. Bedane, S. Derese, L. Brieger, C. Strohmann, M. Spiteller, Anti-inflammatory steroidal sapogenins and a conjugated chalcone-stilbene from *Dracaena usambarensis* Engl, Fitoterapia 146 (2020) 104717, https://doi.org/10.1016/j.fitote.2020.104717.

[50] S.J. Suh, C.H. Kwak, T.W. Chung, S.J. Park, M. Cheeeei, S.S. Park, C.S. Seo, J. K. Son, Y.C. Chang, Y.G. Park, Y.C. Lee, H.W. Chang, C.H. Kim, Pimaric acid from *Aralia cordata* has an inhibitory effect on TNF-α-induced MMP-9 production and HASMC migration via down-regulated NF-κB and AP-1, Chem. Biol. Interact. 199 (2) (2012) 112–119, https://doi.org/10.1016/j.cbi.2012.06.003.

[51] Y. Sun, L. Gao, W. Hou, J. Wu, β-Sitosterol alleviates inflammatory response via inhibiting the activation of ERK/p38 and NF-κB pathways in LPS-exposed BV2 cells, Biomed. Res. Int. 2020 (2020) 7532306, https://doi.org/10.1155/2020/7532306.

[52] L. Shen, S.Q. Zhang, L. Liu, Y. Sun, Y.X. Wu, L.P. Xie, J.C. Liu, Jolkinolide a and Jolkinolide B inhibit proliferation of A549 cells and activity of human umbilical vein endothelial cells, Med. Sci. Monit. 23 (2017) 223–237, https://doi.org/10.12659/msm.902704.

[53] C. Han, Y. Peng, Y. Wang, X. Huo, B. Zhang, D. Li, A. Leng, H. Zhang, X. Ma, C. Wang, Cytotoxic ent-Abietane-type diterpenoids from the roots of *Euphorbia ebracteolate*, Bioorg. Chem. 81 (2018) 93–97, https://doi.org/10.1016/j.bioorg.2018.07.032.

[54] T.K. Vo, Q.T.H. Ta, Q.T. Chu, T.T. Nguyen, V.G. Vo, Anti-hepatocellular-Cancer activity exerted by *β*-Sitosterol and *β*-Sitosterol-glucoside from *Indigofera Zollingeriana* Miq, Molecules 25 (13) (2020) 3021, https://doi.org/10.3390/molecules25133021.

[55] N. Dolai, A. Kumar, A. Islam, P.K. Haldar, Apoptogenic effects of *β*-Sitosterol glucoside from *Castanopsis Indica* leaves, Nat. Prod. Res. 30 (4) (2016) 482–485, https://doi.org/10.1080/14786419.2015.1023201.

[56] S. Sutthivaiyakit, M. Thapsut, V. Prachayasittikul, Constituents and bioactivity of the tubers of *Euphorbia sessiliflora*, Phytochemistry 53 (8) (2000) 947–950, https://doi.org/10.1016/s0031-9422(99)00606-8.

[57] H. Son, J. Kim, Y.K. Shin, K.Y. Kim, Antibacterial activity of pimaric acid against the causative agent of American foulbrood, *Paenibacillus larvae*, J. Apic. Res. 61 (2) (2022) 219–226, https://doi.org/10.1080/00218839.2020.1835250.

[58] L. Pierre Luhata, T. Usuki, Antibacterial activity of β-sitosterol isolated from the leaves of *Odontonema strictum* (Acanthaceae), Bioorg. Med. Chem. Lett. 48 (2021) 128248, https://doi.org/10.1016/j.bmcl.2021.128248.

[59] L. Apaza Ticona, B. Hervás Povo, J. Sánchez Sánchez-Corral, Á. Rumbero Sánchez, Anti-inflammatory effects of TNF- α and ASK1 inhibitory compounds isolated from *Schkuhria pinnata* used for the treatment of dermatitis, J. Ethnopharmacol. 318 (2024) 1–9, https://doi.org/10.1016/j.jep.2023.117051.

[60] L. Apaza Ticona, V. Tena Pérez, A.M. Serban, M.J. Alonso Navarro, A. Rumbero, Alkamides from *Tropaeolum tuberosum* inhibit inflammatory response induced by TNF–α and NF–κB, J. Ethnopharmacol. 235 (2019) 199–205, https://doi.org/10.1016/j.jep.2019.02.015.

[61] L. Apaza Ticona, J. Arnanz Sebastián, A.M. Serban, Á. Rumbero Sánchez, Alkaloids isolated from *Tropaeolum tuberosum* with cytotoxic activity and apoptotic capacity in tumour cell lines, Phytochemistry 177 (2020) 112435, https://doi.org/10.1016/j.phytochem.2020.112435.

[62] L. Apaza Ticona, Á. Rumbero Sánchez, J. Sánchez Sánchez-Corral, P. Iglesias Moreno, M. Ortega Domenech, Anti-inflammatory, pro-proliferative and antimicrobial potential of the compounds isolated from *Daemonorops draco* (Willd.) Blume, J. Ethnopharmacol. 268 (2021) 113668, https://doi.org/10.1016/j.jep.2020.113668.

[63] A. Lundin, T. Bergström, E. Trybala, Screening and evaluation of anti-respiratory syncytial virus compounds in cultured cells, in: Methods in Molecular Biology, Humana Press, Totowa, NJ, 2013, pp. 345–363, https://doi.org/10.1007/978-1-62703-484-5_27.

[64] M. Ekblad, B. Adamiak, T. Bergstrom, K.D. Johnstone, T. Karoli, L. Liu, V. Ferro, E. Trybala, A highly lipophilic sulfated tetrasaccharide glycoside related to muparfostat (PI-88) exhibits virucidal activity against herpes simplex virus, Antivir. Res. 86 (2010) 196–203, https://doi.org/10.1016/j.antiviral.2010.02.318.

[65] E.T. Mahambo, C. Uwamariya, M. Miah, L. da Costa Clementino, L.C. Salazar Alvarez, G.P. Di Santo Metzler, E. Trybala, J. Said, L.H.E. Wieske, J. Ward, K. Rissanen, J.J.E. Munissi, F.T.M. Costa, P. Sunnerhagen, T. Bergström, S. S. Nyandoro, M. Erdelyi, Crotofolane diterpenoids and other constituents isolated from Croton kilwae, J. Nat. Prod. 86 (2023) 380–389, https://doi.org/10.1021/acs.jnatprod.2c01007.